

Syracuse University

## SURFACE

---

Syracuse University Honors Program Capstone Projects    Syracuse University Honors Program Capstone Projects

---

Spring 5-1-2014

# Investigation of Boiling Performance of Graphene-coated Surfaces

Daniel C. Stack

Follow this and additional works at: [https://surface.syr.edu/honors\\_capstone](https://surface.syr.edu/honors_capstone)



Part of the [Applied Mechanics Commons](#), [Energy Systems Commons](#), and the [Heat Transfer, Combustion Commons](#)

---

### Recommended Citation

Stack, Daniel C., "Investigation of Boiling Performance of Graphene-coated Surfaces" (2014). *Syracuse University Honors Program Capstone Projects*. 754.

[https://surface.syr.edu/honors\\_capstone/754](https://surface.syr.edu/honors_capstone/754)

This Honors Capstone Project is brought to you for free and open access by the Syracuse University Honors Program Capstone Projects at SURFACE. It has been accepted for inclusion in Syracuse University Honors Program Capstone Projects by an authorized administrator of SURFACE. For more information, please contact [surface@syr.edu](mailto:surface@syr.edu).

## **Executive Summary**

The advancements driving our society's technological development today are coming from the materials side of research. The discoveries being made in materials science and engineering are changing the parameters of design problems that are hundreds of years old, yielding entirely new solutions that were never feasible or even dreamt of before. With the advent of nanoscale engineering, and the ability to create structures from building blocks one million times smaller than a millimeter, there are seemingly endless possibilities in how humanity will be able to create, improve, and innovate as our understanding of these nanomaterials develops. However, the process to attaining that understanding comes in many small steps. This Capstone Project, which investigates the boiling performance of graphene-coated surfaces, strives to be one such step; it aims to pave the way for improvements in boilers and evaporation systems that play a central role in our everyday lives.

When we think about the phenomenon known as boiling, we generally think of water boiling on a stove to cook pasta or brew tea. What many people do not realize is that boiling is required to generate electricity, refrigerate food, and air condition homes and communities. Boiling is a major process essential to more than 80% of electricity production worldwide, and key to nearly every refrigeration system.

Boiling is the rapid change of liquid to vapor, and occurs when the liquid is heated to its boiling point: the temperature at which the vapor pressure of the liquid is equal to the pressure of the surrounding environment. That is, the

pressure applied by a vapor bubble to its surrounding water equals the pressure of the environment. For example, at  $\sim 100^{\circ}\text{C}$  the vapor pressure of water equals the atmospheric pressure, and boiling can begin. This point is more representative of the moment of impending boiling, and the heat transfer mode is still largely convection, i.e. the transfer of heat by the mixing of colder fluid and warmer fluid. In practice, vapor bubbles begin to form around  $105^{\circ}\text{C}$ , at which point the phenomenon ubiquitously called “boiling” happens; this is the onset of nucleate boiling. In this regime, bubbles nucleate at the interface of water and heated surface, and steadily detach and rise to the top.

As we increase the temperature of the surface, i.e. turn the flame up on our stove, we can increase our heat flux ( $\text{W}/\text{m}^2$ ), or the rate of heat transfer ( $\text{W}$ ) per unit area ( $\text{m}^2$ ), and make the liquid boil faster. The rise of bubbles through the pot of water causes stirring and agitation of the liquid, which is the cause of the improvement in heat flux.

Because the rapid formation and rise of bubbles increases heat flux to our water, we are interested in materials that promote the formation of bubbles. “Hydrophobic” surfaces, i.e. surfaces that repel water, promote the formation of bubbles on a surface. These surfaces resist the movement of water across them, which allows vapor bubbles to nucleate at the surface more freely.

Graphene is a hydrophobic surface that shows great potential as the interfacial surface for boiling processes. Its properties are a result of its unique chemical structure: a sheet of carbon atoms bonded in a 2-D hexagonal, or “honeycomb” lattice, that is only one atom thick. This thickness allows it to attach

to many surfaces by Van der Waals forces, weak intermolecular forces that are only significant at the molecular scale. Graphene is also a very stable structure, which makes it less reactive with other materials. This allows it to resist fouling, a phenomenon that occurs in heat exchangers, where particulates from water and other fluids deposit on the surface, and begin to corrode it and reduce its effectiveness of heat transfer. Because of its greater heat flux potential, ability to attach to most surfaces with just Van der Waals forces, and its resistance to corrosion and fouling, the role of graphene in a boiling heat exchanger stands to be very beneficial.

In my Capstone Project, I sought to test the boiling performance of a graphene-coated surface. Working with Dr. Shalabh C. Maroo and other members of his research group, the Multiscale Research & Engineering Laboratory (MREL), in the Mechanical and Aerospace Engineering Department at Syracuse University, I began my research by transferring graphene from a copper substrate to a SiO<sub>2</sub> wafer, with ITO (indium titanium oxide) on its back. The ITO on the back of the wafer works as a resistance heater, similar to an electric stove, and was used to heat the wafer. The graphene-coated wafer was put in a boiling chamber, and its heat flux was incrementally increased, with surface temperature measurements taken at each increment, up until it reached its “Critical Heat Flux.” This point represents the highest heat flux that can be achieved before the rapid formation of bubbles forms a vapor insulation layer on the heated surface, and any additional temperature increase will cause the system to heat up uncontrollably.

Complementary to the boiling experiments, I measured contact angle of water drops on the surface of the graphene-coated samples. The contact angle is the angle between the flat surface of interest and the line that runs tangent with a drop of water at its point of contact with the surface. Results of the contact angle measurements were used to verify successful transfer and quantify how hydrophobic the samples were. Additionally, I used Raman spectroscopy to analyze the quality of the graphene. Because the unique properties of graphene are dependent on its molecular structure, it is important to know the quality of the graphene, in terms of defects in its 2-D lattice. Raman spectroscopy involves the incidence of a laser of a known energy at the material of interest. When the laser impacts the chemical bonds of the material, it bounces back at a different energy. The way in which the light is shifted in energy determines the types of bonds in the material, and any defects. Because graphene is a very simple structure, Raman spectroscopy is a very powerful tool in determining its quality and detecting defects. This method was used to detect changes in quality before and after the boiling processes. By employing these techniques, boiling curves on graphene-coated surfaces were obtained, and the impact of boiling on graphene was investigated.

## Introduction

Throughout the scientific and engineering communities, graphene has become a substance of seemingly endless possibilities, with applications ranging from structural engineering to corrosion prevention, supercapacitors, and many other technical fields. This Capstone, which investigates the boiling performance of graphene-coated surfaces, aims to pave the way for improvements in boilers and evaporation systems that play a central role in our everyday lives.

When we think about the phenomenon known as boiling, we generally think of water boiling on a stove to cook pasta or brew tea. What many people do not realize is that boiling is required to generate electricity, refrigerate food, and air condition homes and communities. Boiling is a major process essential to more than 80% of electricity production worldwide [1], and key to every refrigeration system.

Boiling is the rapid change of liquid to vapor, and occurs when the liquid is heated to its boiling point: the temperature at which the vapor pressure of the liquid is equal to the pressure of the surrounding environment. For example, at  $\sim 100^{\circ}\text{C}$  the vapor pressure of water equals the atmospheric pressure, and boiling can begin. This point is more representative of the moment of impending boiling, and the heat transfer mode is still largely convection [2]. In practice, vapor bubbles begin to form around  $105^{\circ}\text{C}$ , at which point the phenomenon ubiquitously called “boiling” happens; this is the onset of nucleate boiling. In this regime, bubbles nucleate at the interface of water and heated surface, and steadily

detach and rise to the top. Figure 1 shows the full boiling curve of water, where the onset of nucleate boiling can be seen at point A:

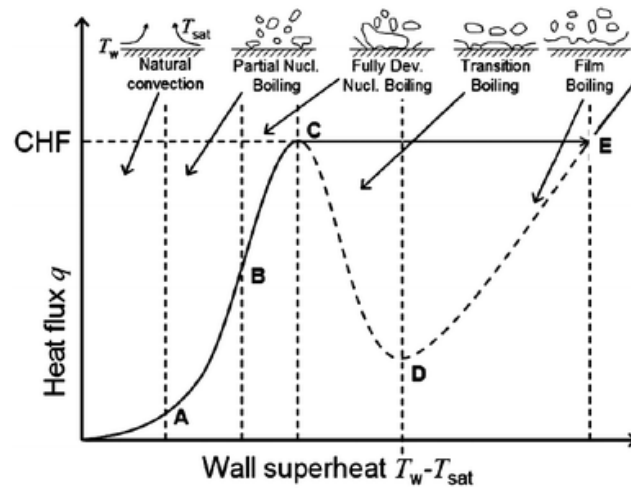


Figure 1: Qualitative boiling curve [2]

As we increase the temperature of the surface, i.e. turn the flame up on our stove, we can increase our heat flux ( $\text{W}/\text{m}^2$ ), or the rate of heat transfer ( $\text{W}$ ) per unit area ( $\text{m}^2$ ), and make the liquid boil faster. The rise of isolated bubbles through the liquid, and subsequent replacement of the bubble with more liquid at its nucleation site, causes agitation of the water that promotes superior heat flux to convection heat transfer. However, as boiling occurs at a greater rate, the rate at which vapor bubbles move away from the surface of our vessel cannot keep up, causing bubbles to begin merging into a vapor layer on the surface. This vapor layer begins to form at point B, where we enter the regime of fully developed nucleate boiling. In this regime, bubbles are no longer isolated, and instead a continuous column of vapor can be seen rising from the surface. This vapor layer on the surface acts as insulation between the liquid and the heating surface. It can be seen that point B is the point of inflection: the point where our increase in heat

flux begins to level off as temperature is increased. If we continue to increase the temperature, the system reaches “Critical Heat Flux,” or CHF, the point at which the heating surface cannot transfer all the heat from the heating source to the liquid due to the insulating vapor layer. It is very dangerous to operate near this point; if the surface is ever to be heated past the temperature of CHF, the drop in the heat flux to the liquid will cause the vessel walls to heat up instead, which will increase its temperature uncontrollably. This heating of the vessel will continue rapidly and may damage or melt the surface. Thus, most commercial systems which incorporate boiling heat transfer operate below the CHF limit.

To enhance nucleate boiling, materials that promote the formation of vapor bubbles on their surfaces are desirable interfaces for boiling. “Hydrophobic” surfaces, i.e. surfaces that repel water, allow for higher rates of heat transfer to the liquid as boiling can be achieved at lower temperatures. Equivalently, a hydrophobic material is said to have low wettability, while a “hydrophilic” material, i.e. a material that attracts water, is said to have high wettability.

A useful concept for both understanding and quantifying wettability is the contact angle which a water droplet makes when placed on the surface. Assuming the surface is level and flat, the contact angle is the angle between the surface and the line that runs tangent with a drop of water at its point of contact with the surface. Contact angle, and hydrophobic and hydrophilic surfaces are depicted in figure 2.

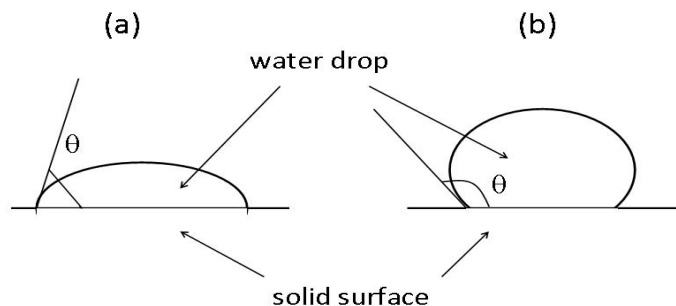


Figure 2: Behavior of hydrophobic and hydrophilic materials [3]

The hydrophobic property of a pure material comes from the competitive molecular forces acting between liquid-material and liquid-liquid. Because water is a polar molecule, the forces between the water-water molecules is much stronger than water-surface molecules causing a water drop to remain in as close contact as possible with itself, and as little in contact with the surface. As a result, water beads up onto the well-defined drops of high contact angle seen in figure 2.

Due to the reduced spreading and movement of water across its surface, hydrophobic surfaces promote formation of vapor nucleation sites achieving higher heat fluxes at lower temperatures. However, by this same token, the hindrance of water movement more readily causes the formation of a vapor film, and results in a lower CHF than a material with high greater water mobility.

Graphene is a hydrophobic material that shows great potential as the interfacial surface for boiling processes. Its properties are a result of its unique chemical structure: a sheet of carbon atoms bonded in a 2-D hexagonal, or “honeycomb” lattice, that is only one atom thick. This lattice is built entirely from covalent bonds, and is nonpolar. Moreover, its molecular structure makes it very stable, and less reactive with materials. As a result, graphene is also resistive to fouling. Fouling is the buildup of unwanted materials on a solid that hinders the

performance of its intended function. This phenomenon, which is a consistent problem in heat exchangers, takes the form of thermally resistant deposits on the exchanger walls, thereby reducing system effectiveness [2]. Graphene shows promise in preventing fouling from occurring in heat exchangers, while also increasing heat flux in boiling processes.

Despite the extensive research in graphene applications today, very little research has been conducted so far to explore the possibilities of graphene as a boiling interface. Indeed, no boiling curve as seen above or CHF has been determined experimentally for graphene-coated surfaces to the best of our knowledge.

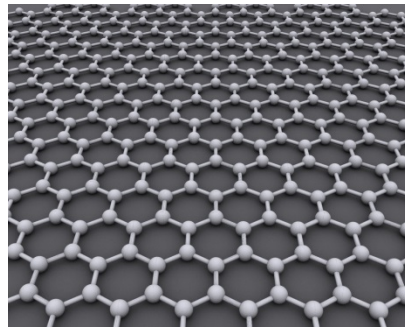


Figure 3: A single sheet of graphene [4]

As previously mentioned, hydrophobic properties arise from a relatively high ratio of cohesive to adhesive forces at the water and material interface. As such, defects in molecular structure stand to influence the behavior of graphene during boiling experiments. Moreover, it is uncertain how boiling will affect the graphene coating. Therefore it is essential to determine the quality of graphene after transfer, and after boiling experiments. Raman spectroscopy techniques have been widely used for graphene characterization, which produce spectra of frequencies associated with the different chemical bonds present in the sample.

Where perfect graphene is uniformly composed of  $sp^2$  bonds, and produces a spectrum with only two noteworthy peaks known as the G and 2D peaks, fabricated graphene will have an additional peak, known as the D peak, which results from boundary layers and lattice defects [5].

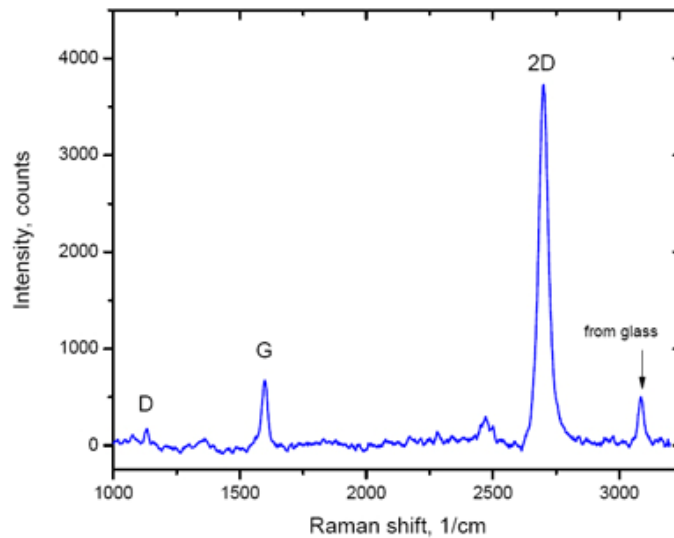


Figure 4: A common Raman spectrum of graphene [5]

The quality of graphene can be quantified by examining the magnitude of this peak relative to the  $sp^2$  peak, or G peak. In turn, the relative magnitude of these peaks will be related and analyzed in terms of the boiling performance and contact angle measurements taken. Additionally, layers of graphene beyond one layer impact Raman spectra by varying the relative intensity of the G and 2D peaks; for greater layers of graphene, the G peak increases in size relative to the 2D peak [6]. Therefore, Raman spectra will also be used to determine that the graphene is largely single layer, and low in defects, as well as how these characteristics change as a result of boiling.



## Methods

### Transfer Considerations

Graphene was purchased as 1"x1" samples grown on 25 $\mu$ m copper foil by chemical vapor deposition (Graphene Supermarket, Calverton, NY). Two common methods of graphene transfer is by spin coating PMMA to the graphene surface, or applying an adhesive tape that loses its adhesion when heated, i.e. thermal release tape. In this experiment graphene is transferred by thermal release tape. While this method of transfer is more prone to discontinuities in the graphene, it is a simpler and more environmentally benign procedure than that required of applying PMMA [7]. In both procedures, the next step entails the etching of the copper substrate.



Figure 5: thermal release tape applied across graphene surface

### Etching Process

Etching was achieved by first firmly applying thermal release tape across the entire surface of graphene using a roller, and then placing the tape-graphene-copper sample, with copper side down, into 38.8% ferric chloride solution (MG Chemicals) at room temperature. The copper foil was allowed to etch in a 100 ml

bath with minimal agitation over the course of approximately one hour. No additional heat was added for the duration, to avoid the production of hazardous fumes. Samples were immersed in deionized (DI) water to remove bulk etchant. They were then immersed in ethanol and isopropanol for 1 minute each, and rinsed thoroughly with DI water until all solutions were removed.

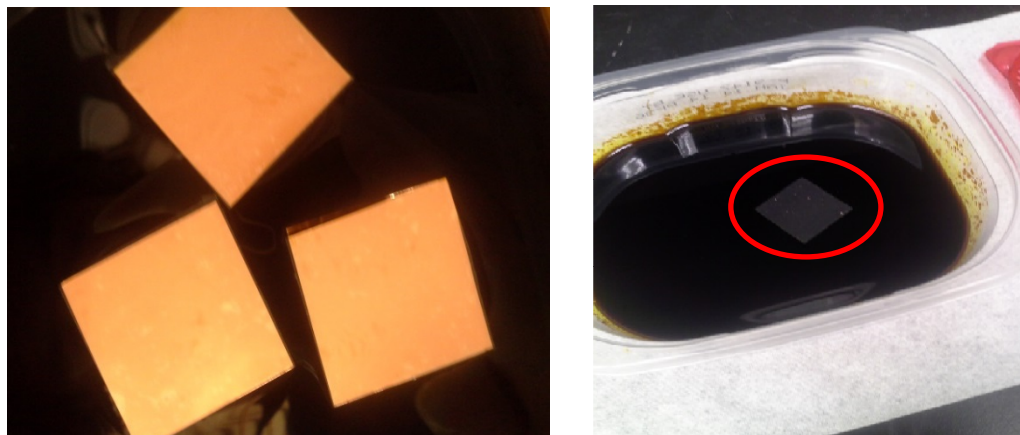


Figure 6: In etchant bath before (left) and after (right)

### **SiO<sub>2</sub> Wafer Cleaning**

For successful graphene transfer from the tape to the SiO<sub>2</sub> wafer, the wafer must be cleaned of organic and inorganic particles as thoroughly as possible. Wafers were washed with acetone, and then immersed in ethanol and isopropanol for 5 minutes each. Wafers were then plasma cleaned at 1050 mTorr for 5 minutes. Wafer cleanliness was verified with static contact angle measurements using a goniometer. Previous wettability experiments have shown SiO<sub>2</sub> to have an advancing contact angle of approximately 42° and a receding contact angle of approximately 10°. Wafers were considered fit for transfer if their contact angles were less than or equal to their advancing contact angle of 42° [8]. Drop size was

approximately 1 $\mu$ l for each measurement. Transfer was completed within 30 minutes of plasma cleaning to minimize deposition of particulates.

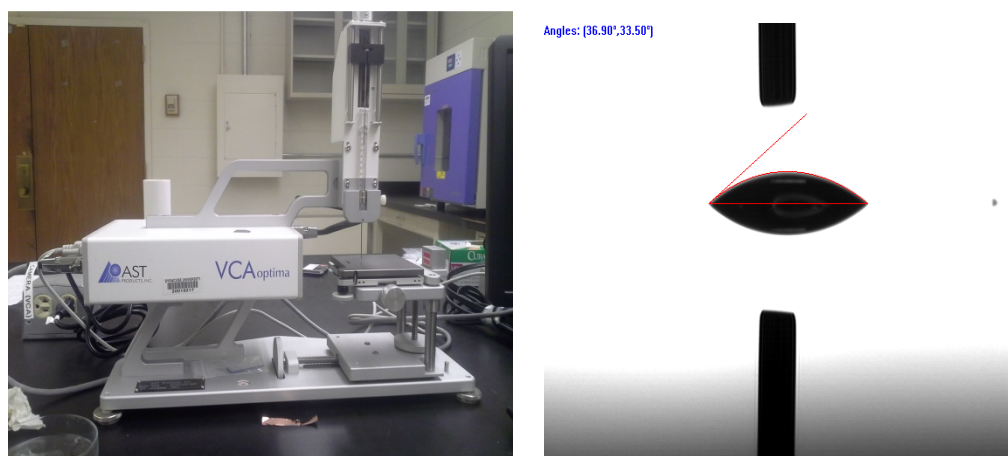


Figure 7: Goniometer (left) and camera-view contact angle of SiO<sub>2</sub> (right)

### Transfer Process

Prior to transfer, the tape-graphene samples were heated in the oven for approximately 5 minutes at 60°C to evaporate remaining DI water. The sample was then firmly pressed, graphene side down, against 2 cm x 2 cm SiO<sub>2</sub> wafer using a roller for even pressure. The tape-graphene-wafer sample was heated in the oven at ~120°C until the tape could be seen to peel away from the wafer (approximately 2 minutes).

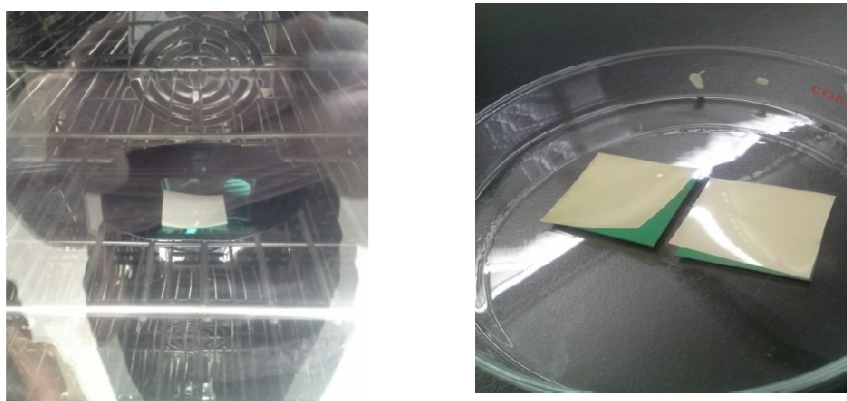


Figure 8: Heating of sample to 120°C (left) and peeling of tape (right)

The success of the transfer was verified with contact angle measurements. Previous wettability experiments have shown single layer graphene on SiO<sub>2</sub> to have an advancing contact angle of approximately 95° and a receding contact angle of approximately 60° [8]. As such, samples with static contact angles consistently within a few degrees of 78° were considered to be successful transfers. Drop size was approximately 1μl for each measurement. Numerous measurements were taken to determine the uniformity of the transfer throughout the sample.

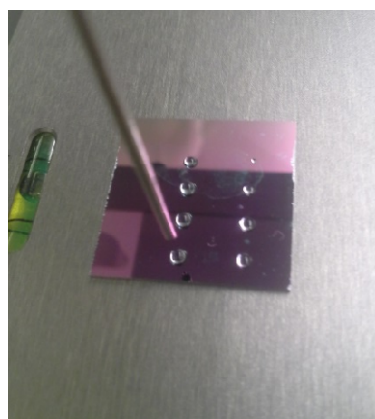


Figure 9: Multiple contact angle measurements on graphene-coated SiO<sub>2</sub>

### **Raman Spectroscopy**

Raman spectra were taken with a Renishaw inVia Raman microscope at Cornell Center for Materials Research (CCMR) at Cornell University, using a 488 nm laser. Spectra were produced from 1200/cm to 2900/cm with an accumulation time of 120 seconds. A 50x objective was used at a spot diameter of 1 μm (0.79 μm<sup>2</sup>).



Figure 10: Renishaw inVia Raman microscope

Sample spectra are used to characterize their quality by examining the ratios of the D and G peaks, and the G and 2D peaks:  $I_D/I_G$  and  $I_{2D}/I_G$ .  $I_D/I_G$  expresses the defects present at the spectrum location, and  $I_{2D}/I_G$  expresses the number of graphene layers at the spectrum location.

### **Boiling Setup and Procedure**

Boiling on the sample surface was controlled by a resistance heater on the underside of the  $\text{SiO}_2$  substrates, which was fabricated before the graphene transfer process. An Zou, a PhD student in the lab, has deposited a  $\sim 100$  nm thick indium tin oxide (ITO) film on the back side of the wafers by physical vapor deposition. Two  $\sim 500$  nm thick patterned copper films ( $1.25$  cm x  $0.625$  cm) were deposited on the ITO surface to be used as electrodes. As the current travels most directly between electrodes, the nominal heating area is  $0.75$  cm x  $1.25$  cm. However, the lateral heat transfer through the Si substrate results in a larger actual boiling area. The methods for calculating the actual boiling area are further detailed in *Zou & Maroo* [9].

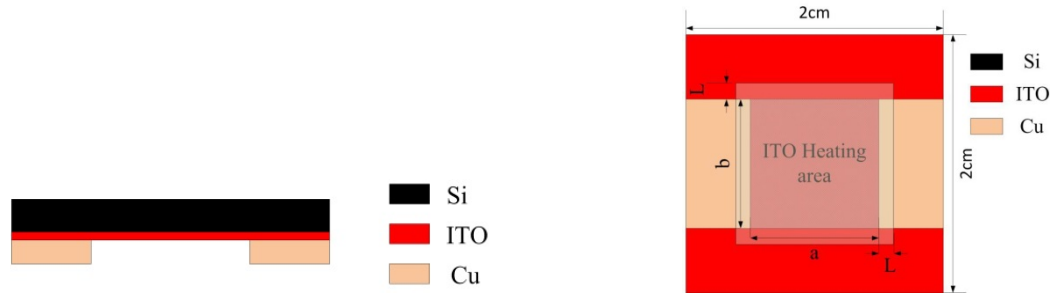


Figure 11: Resistance heater design: side view (left) and bottom view (right). The parameters  $a$ ,  $b$ , and  $L$  are used to calculate the actual boiling area to determine heat flux [9].

The samples were mounted on a platform in a pool boiling chamber present in the lab, of which the setup is shown in figure 11. The setup consists of a liquid chamber and a sample holder where the test sample is placed. Each is made of polycarbonate. An immersion heater was connected to a proportional-integral-derivative (PID) controller to maintain the bulk liquid at saturation temperature, between  $97^{\circ}\text{C}$  and  $100^{\circ}\text{C}$ ; one resistance thermal detector (RTD) was used to monitor and record the bulk temperature near the sample, while another RTD was connected to the PID controller. With the help of An Zou, the test sample was glued to the sample holder using epoxy, which also prevented water leakage and heat loss from the back side of the sample. The wires connecting the sample to the power supply (Agilent 5750A) were soldered on to the copper electrodes. The voltage and current load on the sample were directly monitored by NI DAQ modules. A T-type thermocouple, which was also monitored by a NI DAQ module, was buried in epoxy and was attached to the back side of sample [9].

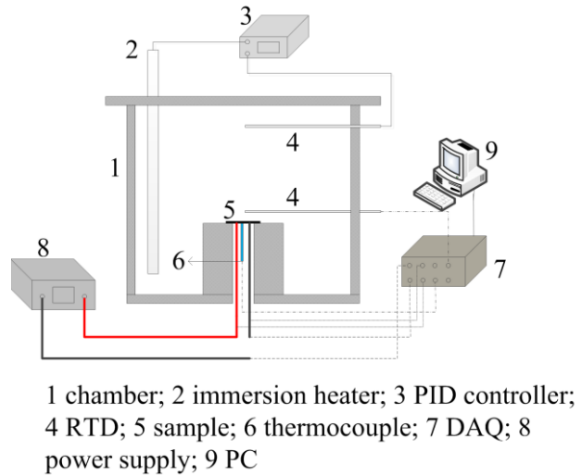


Figure 12: Setup of boiling chamber [9]

Boiling experiments were conducted by An Zou. DI water was degassed prior to each experiment by boiling it in the chamber for one hour with the immersion heater. During the experiment, power supplied to the sample was increased incrementally to produce consecutively higher temperatures. Data were collected only after the sample temperature was observed to vary by no more than  $0.5\text{ }^{\circ}\text{C}$  in a one minute period, and no sooner than 10 minutes after supplied power was increased. Incremental increase was continued until the sample temperature was seen to increase uncontrollably, indicating CHF was reached, and the power was promptly reduced to zero. For more detailed literature on the methods and procedure for boiling data collection, refer to *Zou & Maroo* [9].

## Results and Discussion

Two samples were fabricated, analyzed and tested as described in the methods section. Following graphene transfer, each sample was tested for contact angle in eight different locations, in the configuration shown in figure 13, the results of which can be seen in figure 14 and 15.

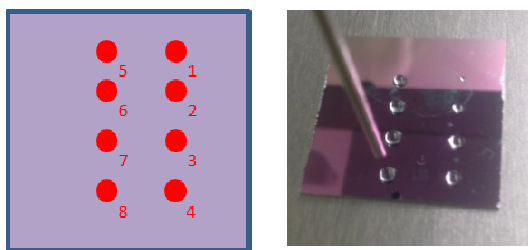


Figure 13: Contact angle measurement locations of each sample

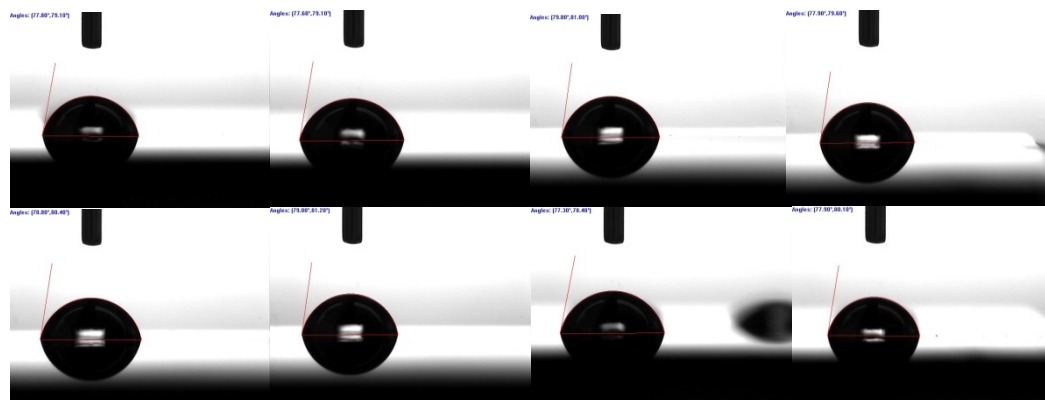


Figure 14: Sample 1 contact angle. Locations 1-8 (from top left to bottom right). All angles between  $77^\circ$  and  $82^\circ$

Sample 1 contact angle measurements were consistent with that of the average of the receding and advancing contact angle of  $78^\circ$  detailed in earlier work [8].

Throughout the sample, contact angle ranged from  $77^\circ$  to  $82^\circ$ , comfortably within the expected range of  $95^\circ$  and  $60^\circ$ .

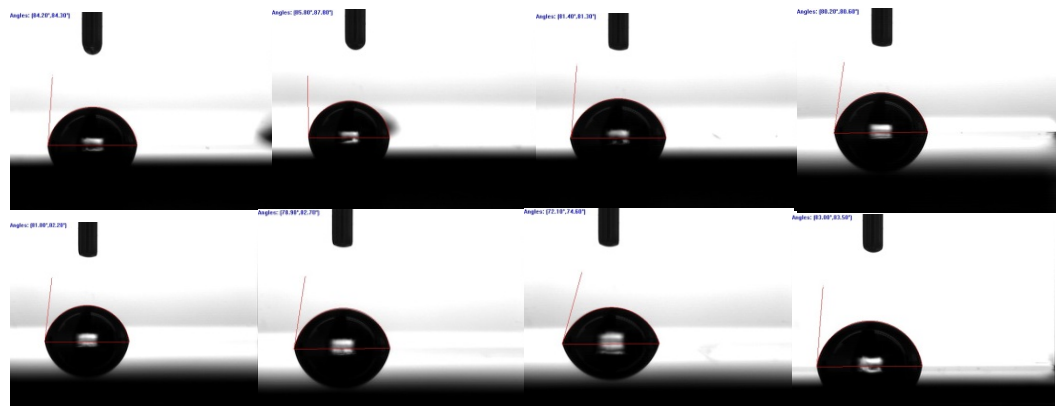


Figure 15: Sample 2 contact angle. Locations 1-8 (from top left to bottom right). All angles between  $72^\circ$  and  $88^\circ$

Sample 2 measurements (figure 15) had a larger deviation from the average contact angle, with a range from  $72^\circ$  to  $88^\circ$ . This is still well within the expected angle range. Given the results, the otherwise hydrophilic  $\text{SiO}_2$  was unmistakably covered with a hydrophobic coating following removal of the transfer tape; the graphene transfer was determined to be successful for both samples.

Following confirmation of transfer, Raman spectra of each sample were taken with the Renishaw inVia microscope at CCMR at Cornell University. Six and three raman spectra were obtained for samples 1 and 2, respectively. For each sample, the microscope coordinate origin was set at a selected reference corner, and used for Raman measurements before and after the boiling experiment, to ensure comparison of the same locations. It is important to note that returning to the exact same spot is not practically achievable due to the error in setting the origin before and after the boiling experiments. Locations are within  $\sim 100 \mu\text{m}$  of one another. Following the establishment of the origin, coordinates were inputted for precise movement to the desired location. The Raman spectra locations are shown in the Cartesian coordinate systems shown in figure 16.

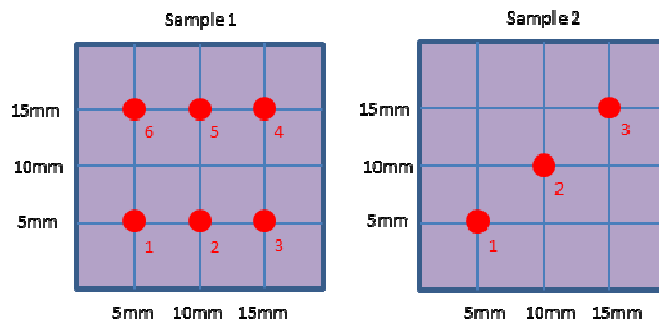


Figure 16: Raman spectra locations, before and after boiling experiment

The goal of the spacing selected was to gain evenly distributed spectra for a more comprehensive profile of each sample. Figure 17 shows the resulting spectra of each sample.

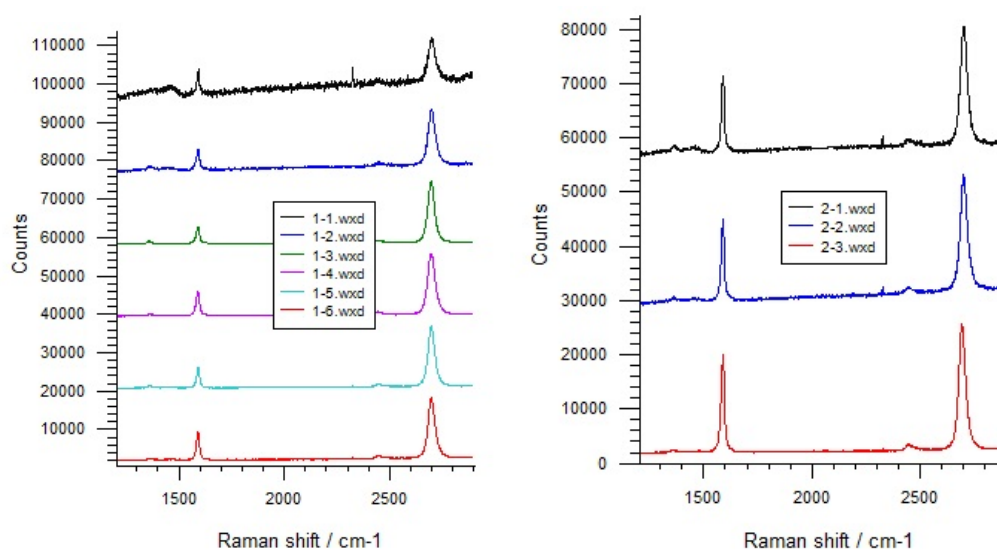


Figure 17: Raman spectra before boiling: sample 1 (left) and sample 2 (right)

Pre-boiling Raman spectra were found to be largely consistent across each sample. The D peak, G peak, and 2D peak locations of all spectra were at approximately  $1352$ ,  $1585$ , and  $2703$   $\text{cm}^{-1}$ , deviating by no more than 3, 2, and 4  $\text{cm}^{-1}$ , respectively. In terms of peak intensities, sample results differed noticeably, specifically in the ratio of  $I_{2D}/I_G$ . Results are summarized in table 1.

Pre-Boiling Spectra Summary		
Sample 1		
Location	D/G	2D/G
1-1	-	1.48
1-2	0.18	2.94
1-3	0.16	3.64
1-4	0.07	2.47
1-5	0.10	2.93
1-6	0.08	2.10
Sample 2		
Location	D/G	2D/G
2-1	0.12	1.52
2-2	0.07	1.41
2-3	0.03	1.28

Table 1: Raman spectra before boiling experiment: relative peak intensities

While some discrepancies exist among the spectra of different studies, a majority of sources [10] [6] [11] agree that an  $I_{2D}/I_G$  of 2 is the characteristic ratio of single layer graphene, and an  $I_{2D}/I_G$  of 1 is the characteristic ratio of bilayer graphene, for both 532 nm and 488 nm excitation. With the exception of 1-1, sample 1 showed an  $I_{2D}/I_G$  above 2 for all tested locations of the surface, reaching a ratio as high as 3.64 at location 1-3. Comparatively, sample 2 fell short of  $I_{2D}/I_G$  by a significant margin, reaching as high as 1.52 and as low as 1.28. Where  $1 < I_{2D}/I_G < 2$ , it is possible that sample 2 experienced partial folding or overlapping of graphene during the transfer process, which resulted in a weighted averaging of bilayer and single layer spectra. Though this may have implications in terms of adherence of the graphene to the  $\text{SiO}_2$  substrate, the difference in wettability of single layer and bilayer graphene has been shown to be negligible [8]. In the case of both sample 1 and 2, the ratio of the D peak and G peak,  $I_D/I_G$ , never exceeded 0.18. This comfortably satisfies the metric of quality used by the manufacturer

Graphene Supermarket, whose own Raman spectra are used to verify that products have an  $I_D/I_G$  of no more than 0.3. The one location whose defects may exceed this limit is 1-1, whose defect peak was indeterminate within an anomalous region. If  $I_D/I_G$  was measured using the intensity at 1350, an  $I_D/I_G$  of approximately 0.3 would be the result. In summary, the pre-boiling Raman spectra indicated uniform transfer of high quality graphene, with potentially homogeneous folding and overlapping of graphene into bilayer sites on sample 2.

Boiling experiments were run for each sample by An Zou. Figure 18 shows the result of sample 1.

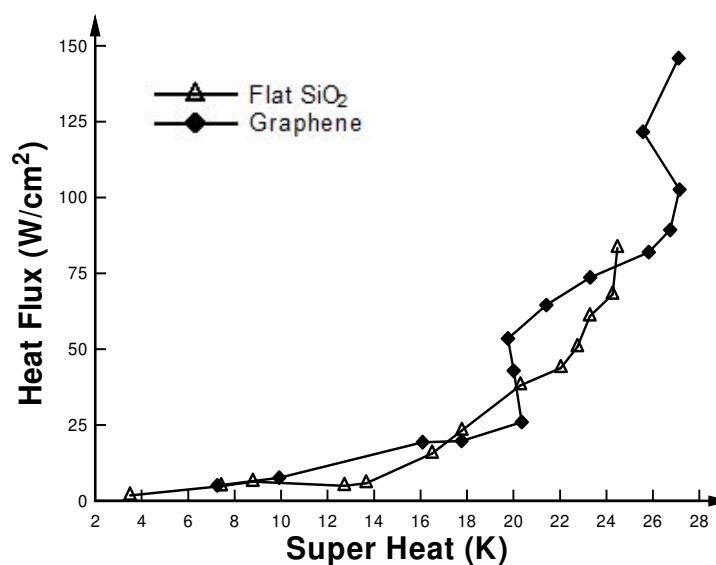


Figure 18: Sample 1 boiling experiment results

Sample 1 exhibited highly unusual and unexpected behavior during the experiment due to water leakage around the sample.. At 20 °C and 22 °C, graphene heat flux exceeds SiO<sub>2</sub> heat flux by 13 W/cm<sup>2</sup> and 25 W/cm<sup>2</sup>, or 33% and 56%, respectively. This is to be expected from the low wettability of the graphene surface. However, as stated earlier, this increased heat transfer

coefficient at lower relative temperatures would expectedly come with the tradeoff of a lower CHF, due to the promotion of vapor film formation. Instead, the sample is seen to exceed the critical point of the hydrophilic SiO<sub>2</sub>, both in temperature and CHF, reaching a value of almost 150 W/cm<sup>2</sup> at a temperature of 27 °C above saturation. A 76% increase over the CHF of blank SiO<sub>2</sub> was most probably water leaking onto the backside of the sample leading to the increased power consumption by water evaporation. Sample 2 showed performance characteristics, shown in figure 19.

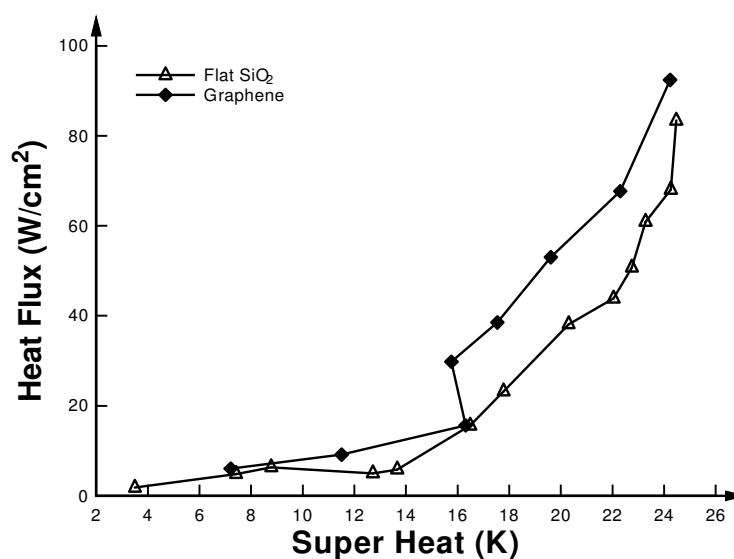


Figure 19: Sample 2 boiling experiment results

The sample again had a greater heat transfer coefficient than SiO<sub>2</sub>, with a 15 W/cm<sup>2</sup> increase over SiO<sub>2</sub> from 16 °C through 22 °C. However, the expected performance of a purely hydrophobic material is again contradicted at the CHF, the onset of which occurred at the same temperature as SiO<sub>2</sub>, at a value of 93 W/cm<sup>2</sup>, 9% greater than SiO<sub>2</sub>. No water leak was observed in this sample.

Both samples exhibited behavior more complex than a uniform and constant hydrophobic surface, suggesting that surface properties changed with

time over the course of the boiling experiment. To produce a CHF higher than  $\text{SiO}_2$ , surface wettability would have had to be relatively high. Conversely, to achieve a heat transfer coefficient significantly higher than  $\text{SiO}_2$  at lower temperatures, wettability must have been relatively low.

The Raman spectra taken after the boiling experiments provide more insight into the sample performance. Figure 20 shows the post-boiling Raman spectra from the same nine locations characterized before the boiling experiments.

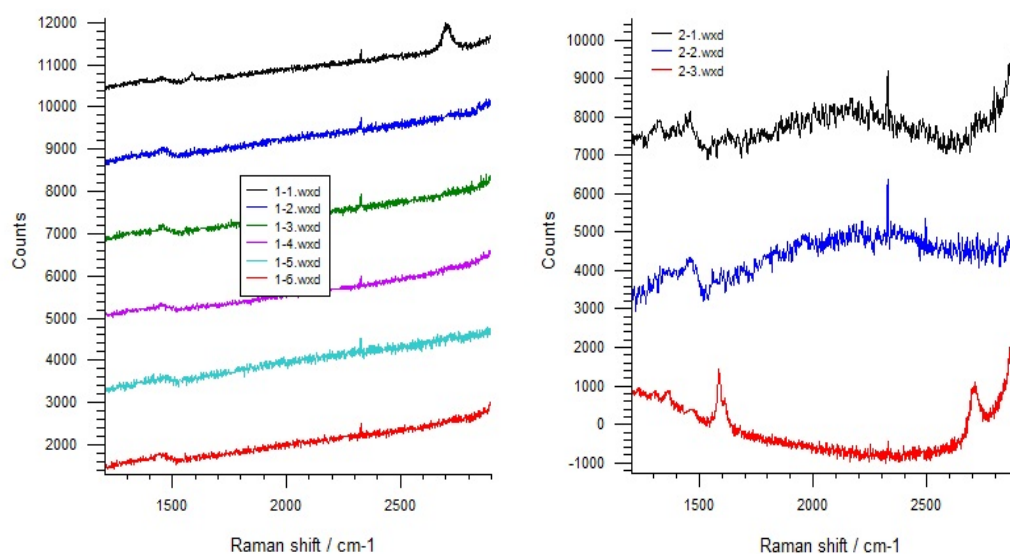


Figure 20: Raman spectra after boiling: sample 1 (left) and sample 2 (right)

As seen in the post-boiling Raman spectra, nearly all of the graphene previously found in these locations has been destroyed. The only exceptions are found at 1-1 and 2-3. Each peak is dramatically less intense than previously found, suggesting that the  $0.79 \mu\text{m}^2$  spot area is not uniformly covered by graphene. Peak comparisons are shown in table 2.

Post-Boiling Spectra Summary		
Sample 1		
Location	D/G	2D/G
1-1	-	3.20
1-2	-	-
1-3	-	-
1-4	-	-
1-5	-	-
1-6	-	-
Sample 2		
Location	D/G	2D/G
2-1	-	-
2-2	-	-
2-3	0.23	1.04

Table 2: Raman spectra after boiling experiment: relative peak intensities

The  $I_{2D}/I_G$  of 1-1 is found to be in excess of 3, which is significantly higher than the  $I_{2D}/I_G$  of 1.48 at that location before boiling. In contrast, the  $I_{2D}/I_G$  of 2-3 is the lowest of any spectrum, at only 1.04. Additionally, the  $I_D/I_G$  of 2-3 is 0.23, signifying large defects relative to previous spectra. If the  $I_D/I_G$  of 1-1 were to be evaluated from the intensity around  $1350\text{ cm}^{-1}$ , it would be evaluated as 1.0. In observing these two cases, boiling appears to have a detrimental impact on graphene quality and an inconsistent impact on the number of graphene layers present. Most prominently, these two cases have shown the boiling process to largely destroy the graphene at the interface.

Based on the experimental results and sample characterization, the most likely explanation for the boiling curves produced is the destruction of graphene over the course of each boiling experiment. Though the Raman spot size is small, it is with reasonable certainty due to the spacing of spectra taken as well as the large array of contact angle measurements taken that both samples were covered

in uniform, high quality, single layer (and partially bilayer) graphene. Then, in both boiling curves, it can be seen without mistake the behavior of a hydrophobic surface, in the form of high heat transfer coefficient and greater heat fluxes at each point relative to SiO<sub>2</sub>. Towards the end of each boiling trial, behavior of a hydrophilic surface is exhibited, in the form of higher CHF. This transition from one behavior to the other is explained by loss and destruction of graphene over the course of the experiment.

However, it would not be possible to achieve CHF higher than blank SiO<sub>2</sub> if by the end of the experiment only blank SiO<sub>2</sub> remained. Instead, the remaining graphene on each sample at the point of CHF must be attributed to the superior CHF. Indeed, the explanation that hydrophobic and hydrophilic surfaces interacted to produce greater heat transfer coefficient and higher CHF is consistent with results of studies. Engineering of surfaces with hydrophobic and hydrophilic interactions have been shown to promote higher CHF with “hydrophobic networks and hydrophobic islands,” with heat fluxes of 190 W/cm<sup>2</sup> reported by Betz, Xu, Qiu, & Attinger [12]. The apparently small amount of graphene remaining on each sample would perceivably create a similar interaction at the end of each boiling experiment. The interaction between traces of hydrophobic graphene and the exposed hydrophilic SiO<sub>2</sub> is therefore the most likely explanation for the results seen in the experiment. However, further experiments are required to prove/disprove this conclusion as the dataset of two graphene coated samples is insufficient.

## Conclusion

The outcome of this experiment has shown some of the first insight into how boiling on graphene-coated surfaces can dramatically alter the boiling curve of the surface it covers, and the immense potential graphene has to enhance boiling performance in both heat transfer coefficient and CHF, given the proper configuration. From a graphene quality perspective, the performance of the graphene transfer method was validated by contact angle measurements and Raman characterization as a simple and effective means to fabricate graphene-coated samples. Moreover, Raman characterization was validated as an invaluable tool for explaining the behavior of the graphene-coated samples before and after the boiling experiment. The experiment outcome also reveals key areas of difficulty that must be investigated further in future testing. The very different boiling curves produced by both samples and the uncontrolled loss of graphene during the experiment are essential problems that must be addressed moving forward.

Given what has been learned from this experiment, further heat transfer experimentation that involves more incrementally controlled processes and frequent surface characterization would help clarify the nature of graphene loss on samples. Running these experiments with different transfer techniques may reveal that, from a preservation perspective, PMMA or more sophisticated tape transfer techniques allow for a tighter, stronger attractive force between graphene and substrate, more capable of resisting boiling conditions. In any case, more samples must be fabricated and tested before stronger conclusions can be drawn.

## Bibliography

1. *World Energy Outlook 2013*. International Energy Agency.
2. Cengel, Ghajar. *Heat and Mass Transfer: Fundamentals & Applications*. 4<sup>th</sup> Ed. McGraw Hill. 2011. Chapter 10.
3. Piccirillo, Clara. *Pickering Emulsions and Equilibrium Time: Kinetic Study*. Jan 16 2012. <http://www.decodedscience.com/pickering-emulsions-and-equilibrium-time-kinetic-study/9538/2>
4. Wikipedia. *Graphene*. 2014.  
<http://en.wikipedia.org/wiki/File:Graphen.jpg>
5. Graphene Supermarket. *Frequently Asked Questions about Graphene Grown via Chemical Vapor Deposition*.  
[http://graphenesupermarket.com/White\\_Papers/CVDGrapheneFAQ.pdf](http://graphenesupermarket.com/White_Papers/CVDGrapheneFAQ.pdf)
6. Isaac Childres, Luis A Jaeger, Wonjun Park, Helin Cao, and Yong P. Chen. *Raman Spectroscopy of Graphene and Related Materials*. Purdue University.
7. Graphene Supermarket. *Graphene Transfer Guide*. <https://graphene-supermarket.com/Graphene-Transfer-Guide.html>
8. Rishi Raj, Shalabh C. Maroo, and Evelyn N. Wang. *Wettability of Graphene*. *Nano Letters*, 2013 13 (4), March 4, 2013, 1509-1515, DOI: 10.1021/nl304647t
9. Zou, An and Maroo, Shalabh C., *Critical height of micro/nano structures for pool boiling heat transfer enhancement*. *Applied Physics Letters*, 103, 221602 (2013), DOI:<http://dx.doi.org/10.1063/1.4833543>

10. I. Calizo, A. A. Balandin, W. Bao, F. Miao, and, and C. N. Lau.  
*Temperature Dependence of the Raman Spectra of Graphene and Graphene Multilayers.* Nano Letters 2007 7 (9), 2645-2649 DOI: 10.1021/nl071033g
11. Wall, Mark. The Raman Spectroscopy of Graphene and the Determination of Layer Thickness. Thermo Fischer Scientific. 52252. 2011
12. Betz, Amy Rachel and Xu, Jie and Qiu, Huihe and Attinger, Daniel. *Do surfaces with mixed hydrophilic and hydrophobic areas enhance pool boiling?* Applied Physics Letters, 97, 141909 (2010), DOI:<http://dx.doi.org/10.1063/1.3485057>